

Constraining Parameters for the Accelerating Universe in $f(R, \mathcal{L}_m)$ Gravity

Y. Kalpana Devi^{1,*}, S.A. Narawade^{1,†} and B. Mishra^{1,‡}

¹*Department of Mathematics, Birla Institute of Technology and Science-Pilani,
Hyderabad Campus, Hyderabad-500078, India.*

(Dated: July 16, 2024)

Abstract: In the paper, we present an accelerating cosmological model in $f(R, \mathcal{L}_m)$ gravity with the parameter constrained through the cosmological data sets. At the beginning, we have employed a functional form of $f(R, \mathcal{L}_m) = \frac{R}{2} + \alpha R^2 + \mathcal{L}_m^\beta$, where α and β are model parameters. This model is well motivated from the Starobinsky model in $f(R)$ gravity and the power law form of $f(\mathcal{L}_m)$. The Hubble parameter has been derived with some algebraic manipulation and constrained by Hubble data and Pantheon⁺ data. With the constraint parameters, present value of deceleration parameter has been obtained to as $q_0 \approx -0.63$ with the transition at $z_t \approx 0.7$. It shows the early deceleration and late time acceleration behaviour. The present value of other geometric parameters such as the jerk and snap parameter are obtained to be $j_0 \approx 0.78$ and $s_0 \approx 0.1$ respectively. The state finder diagnostic test gives the quintessence behaviour at present and converging to Λ CDM at late times. Moreover the $Om(z)$ diagnostics gives negative slope which shows that the model favours the state finder diagnostic result. Also the current age of Universe has been obtained as, $t_0 = 13.64$ Gyrs. The equation of state parameter also shows the quintessence behaviour. Based on the present analysis, it indicates that the $f(R, \mathcal{L}_m)$ gravitational theory may be another alternative to study the dark energy models.

Keywords: $f(R, \mathcal{L}_m)$ gravity, Accelerating Universe, Hubble data, Pantheon⁺ data, $Om(z)$ Diagnostics.

I. INTRODUCTION

In gravitational interactions, General Relativity (GR) is the most commonly used theory. Levi-Civita has been used to describe gravity by using Riemannian geometry. Space time is measured by Ricci curvature R and the geometry is nonmetricity-free and torsion-free. Astrophysical observations from supernovae of type Ia [1–3], cosmic microwave background anisotropies [4–8], large scale structure [9–11], baryon acoustic oscillations [12], and weak lensing [13] indicate that in the present epoch, the Universe is accelerating. The most promising feature of the Universe is the dominance of exotic energy component with large negative pressure, known as dark energy (DE). In general, the research devoted to modifying and extending GR has two main motivations: (i) the modified gravity hypothesis is based on cosmological grounds, and it is an effective explanation for the expansion of the Universe over time [14, 15] and; (ii) for purely theoretical reasons. In order to achieve a quantum gravity theory [16], it intends to enhance renormalizability of the GR. As described in [2, 6, 12, 17–20] the observed

accelerated expansion of the Universe has been modeled by the cosmological constant Λ . There have been numerous challenges to the Λ CDM (Cold Dark Matter) cosmological model. To explain the role of DE in cosmic acceleration, a number of alternative models have been proposed using general relativity (GR). One of the approach is, by replacing scalar curvature R by an arbitrary function R in Einstein-Hilbert action, referred as $f(R)$ gravity.

$f(R)$ theory of gravity one of the most viable and realistic theory among the various modifications of GR. It is considered as one of the most cosmologically important theory due to its higher order curvature invariant models. The late time cosmic expansion behaviour of the Universe can also be explained by $f(R)$ theory [21]. Since it has been shown in [17] that $f(R)$ theory is equivalent to scalar-tensor theory, it is incompatible with solar system tests under weak fields. Nevertheless some models that also satisfies the solar system test are also discussed in [22–24]. It is also discussed in Capozziello et al. [25] that the matter dominating and dark energy dominating phases can be achieved from a $f(R)$ power law cosmological model. Various cosmological models shows the unification of early time inflation and late time cosmic acceleration [26–29]. It can also describe the phase transition of the Universe from deceleration to acceleration. Energy conditions to locally homogeneous and isotropic Universe in $f(R)$ gravity have been discussed in [30]. For such certain reasons $f(R)$ theory has attract considerable interest.

* kalpanayengkhom123@gmail.com

† shubhamn2616@gmail.com

‡ bivu@hyderabad.bits-pilani.ac.in

$f(R, \mathcal{L}_m)$ theory of gravity arises from an extension from $f(R)$ theory with an explicit coupling between matter Lagrangian density (\mathcal{L}_m) and the Ricci scalar (R). It was purposed in [31] and found out that the motion of a test particle was non-geodesic and an extra force arises orthogonal to the four-velocity due to the coupling. The physical implications of such force have been discussed under a generalized gravity model with an arbitrary coupling between the matter Lagrangian density and Ricci scalar [32]. A more generalized study is done by considering the gravitational Lagrangian as a function of Ricci scalar R and matter Lagrangian density \mathcal{L}_m in [33]. It is one of the most extended theory with the background of Riemann geometry. Various impacts of the non-minimal matter-geometry coupling on astrophysical and cosmological scenarios have been discussed in [34–39]. The non-geodesic equation of motion of the particles due to the additional force can lead to significant modification on the cosmological behaviour. The extra force has impact on the trajectory of the particles and it can potentially explain the accelerated expansion of the Universe without involving the dark matter term. It can also effect the expansion history of the Universe, alter the cosmic growth rate and structure formation. So it can be helpful to study such effects and understand the viability and implication of $f(R, \mathcal{L}_m)$ gravity.

The article has been discussed in various sections as follows.: In Section II we have derived the equation of motion for spatially flat FLRW spacetime geometry in $f(R, \mathcal{L}_m)$ gravity and introduced the $H(z)$ parameterization. Then, we have done the statistical analysis of the numerical solution for Hubble parameter with Monte Carlo Markov Chain (MCMC) simulation and obtained the constrained free model parameters using observational datasets in Section III. Using the constrained free model parameter values we studied the behaviour of cosmographic parameter in Section IV. In Section V we have performed various tests to check the validation of model containing the state finder diagnostics and the $Om(z)$ diagnostics. The results obtained and the conclusions are given in Sec.VI.

II. MATHEMATICAL FORMALISM

The action for $f(R, \mathcal{L}_m)$ gravity [33],

$$S = \int d^4x \sqrt{-g} f(R, \mathcal{L}_m), \quad (1)$$

where g , R and \mathcal{L}_m be respectively the metric determinant, Ricci scalar and matter Lagrangian; $8\pi G = 1$. Applying the variational principle in Eq. (1), one can obtain the field equations of $f(R, \mathcal{L}_m)$ gravity as,

$$R_{\mu\nu} f_R + (g_{\mu\nu} \nabla_\mu \nabla^\mu - \nabla_\mu \nabla_\nu) f_R - \frac{f}{2} g_{\mu\nu} = \frac{1}{2} f_{\mathcal{L}_m} (T_{\mu\nu} - \mathcal{L}_m g_{\mu\nu}). \quad (2)$$

For brevity, we represent $f \equiv f(R, \mathcal{L}_m)$, $f_R \equiv \partial f(R, \mathcal{L}_m) / \partial R$ and $f_{\mathcal{L}_m} \equiv \partial f(R, \mathcal{L}_m) / \partial \mathcal{L}_m$. We consider, $f(R, \mathcal{L}_m) = f_1(R) + f_2(R)G(\mathcal{L}_m)$, where $f_1(R)$ and $f_2(R)$ are arbitrary function of Ricci scalar and $G(\mathcal{L}_m)$ is a function of matter Lagrangian density. When $f_1(R) = 1$, $f_2(R) = 1$ and $G(\mathcal{L}_m) = \mathcal{L}_m$, Eq. (2) reduces to the field equations of General Relativity (GR) whereas for $f_2(R) = 1$ and $G(\mathcal{L}_m) = \mathcal{L}_m$ it reduces to that of $f(R)$ gravity. Moreover, for linear coupling of matter and geometry, $G(\mathcal{L}_m) = 1 + \lambda \mathcal{L}_m$, where λ is a constant. Now, the contracting form of Eq. (2) can be written as,

$$f_R R + 3 \nabla_\mu \nabla^\mu f_R - 2f = f_{\mathcal{L}_m} \left(\frac{1}{2} T - 2\mathcal{L}_m \right). \quad (3)$$

From Eq. (2) and Eq. (3), one can eliminate the term $\nabla_\mu \nabla^\mu f_R$ and the resulting equation becomes,

$$f_R \left(R_{\mu\nu} - \frac{1}{3} R g_{\mu\nu} \right) + \frac{f}{6} - \nabla_\mu \nabla_\nu f_R = \frac{1}{2} f_{\mathcal{L}_m} \left(T_{\mu\nu} - \frac{1}{3} (T - \mathcal{L}_m) g_{\mu\nu} \right). \quad (4)$$

Taking the covariant divergence of Eq. (2), with the use of the following mathematical identity

$$\nabla^\mu \left[R_{\mu\nu} f_R + (g_{\mu\nu} \nabla_\mu \nabla^\mu - \nabla_\mu \nabla_\nu) f_R - \frac{f}{2} g_{\mu\nu} \right] = 0, \quad (5)$$

one can obtain the divergence of energy-momentum tensor $T_{\mu\nu}$ as,

$$\begin{aligned} \nabla^\mu T_{\mu\nu} &= \nabla^\mu \ln[f_{\mathcal{L}_m}] (\mathcal{L}_m g_{\mu\nu} - T_{\mu\nu}), \\ &= 2 \nabla^\mu \ln[f_{\mathcal{L}_m}] \frac{\partial \mathcal{L}_m}{\partial g^{\mu\nu}}. \end{aligned} \quad (6)$$

The requirement of the conservation of the energy-momentum tensor of matter ($\nabla^\mu T_{\mu\nu} = 0$) provides an effective functional relation between the matter and Lagrangian density. Moreover, the conservation of the energy-momentum tensor yields

$$\nabla^\mu \ln f_{\mathcal{L}_m} = 0. \quad (7)$$

We consider the FLRW space-time as,

$$ds^2 = -dt^2 + a^2(t) \left(dr^2 + r^2 d\theta^2 + r^2 \sin^2 \theta d\phi^2 \right), \quad (8)$$

where $a(t)$ is the scaling factor with cosmic time t . The stress energy-momentum tensor for a perfect fluid can be written as,

$$T_{\mu\nu} = (p + \rho)u_\mu u_\nu + p g_{\mu\nu}, \quad (9)$$

where u_μ is the four velocity vectors along the time directions, ρ is the matter energy density and p is the isotropic pressure; u_μ satisfy the relations $u_\mu u_\nu g^{\mu\nu} = -1$. Using Eq. (8) and Eq. (9) in Eq. (2), the field equations of $f(R, \mathcal{L}_m)$ gravity can be obtained as,

$$\begin{aligned} 3H^2 f_R + \frac{1}{2}(f - f_R R - f_{\mathcal{L}_m} \mathcal{L}_m) + 3H \dot{f}_R &= \frac{1}{2} f_{\mathcal{L}_m} \rho, \\ \dot{H} f_R + 3H^2 f_R - \ddot{f}_R - 3H \dot{f}_R + \frac{1}{2}(f_{\mathcal{L}_m} \mathcal{L}_m - f) &= \frac{1}{2} f_{\mathcal{L}_m} p, \end{aligned} \quad (10)$$

where the Hubble parameter, $H = \frac{\dot{a}}{a}$. To solve the system [Eq. (10)], we need to define a well motivated form of $f(R, \mathcal{L}_m)$. Since $f(R, \mathcal{L}_m) \rightarrow f(R) + f(\mathcal{L}_m)$, we consider $f(R) = R + \alpha R^2$ [40] with a coefficient of $(1/2)$ in the ' R ' term such that the resulting equations of motion correctly reduces to General Relativity under certain limits and $f(\mathcal{L}_m) = \mathcal{L}_m^\beta$ inspired from power law model which shows similar background to Λ CDM for small value and redshift and deviates slowly with increase in redshift [41]. Hence the form becomes

$$f(R, \mathcal{L}_m) = \frac{R}{2} + \alpha R^2 + \mathcal{L}_m^\beta, \quad (11)$$

so that $f_R = \frac{\partial f(R, \mathcal{L}_m)}{\partial R} = \frac{1}{2} + 2\alpha R$, $f_{RR} = \frac{\partial f_R}{\partial R} = 2\alpha$, $\dot{f}_R = \frac{\partial f_R}{\partial t} = 2\alpha \dot{R}$ and $f_{\mathcal{L}_m} = \beta \mathcal{L}_m^{\beta-1}$, where α and β are constants and are to be constrained in order to get the accelerating behaviour. Considering $\mathcal{L}_m = \rho$ and the barotropic fluid $p = \omega\rho$ for a homogeneous and isotropic Universe and using Eq. (11), the first Friedmann equation becomes,

$$\frac{3}{2}H^2 + 108\dot{H}H^2\alpha + 36\ddot{H}H^2\alpha - 18\dot{H}^2\alpha = (\beta - \frac{1}{2})\rho^\beta. \quad (12)$$

One can check that, Eq. (12) reduces to GR field equations when $\alpha = 0$ and $\beta = \frac{1}{2}$. Further we can express Eq. (12) as a function of redshift using the relation,

$$-dz = (1+z)H(z)dt, \quad (13)$$

so that $\dot{H} = -(1+z)H(z)\frac{dH}{dz}$ and $\ddot{H} = (1+z)^2 H^2(z)\frac{\partial^2 H}{\partial z^2} + (1+z)^2 H(z)\left(\frac{\partial H}{\partial z}\right)^2 + (1+z)H^2(z)\frac{\partial H}{\partial z}$.

Subsequently, Eq. (12) reduces to a second-order non-linear differential equations as,

$$\begin{aligned} H'' + \frac{(2H-1)}{2H^2}(H')^2 + \frac{(H-3)}{H(1+z)}H' \\ - \frac{\left(\beta - \frac{1}{2}\right) \left(3(H_0)^2(1+z)^3 \Omega_{m0}\right)^\beta - \frac{3}{2}(H)^2}{24H^2(1+z)^2\alpha} = 0. \end{aligned} \quad (14)$$

where prime ('') denotes the derivative in redshift, H_0 be the present value of the Hubble parameter and Ω_{m0} denotes the present density parameter for matter dominated phase and the radiation era case is neglected in the further analysis. Now, we shall solve Eq. (14) numerically to find the Hubble parameter so that the dynamical parameters and other geometrical parameters of the models can be analysed.

III. THE COSMOLOGICAL DATASETS AND THE CONSTRAINED PARAMETERS

In this study we use Hubble and Hubble+Pantheon⁺ datasets to constrained the model parameters using Markov Chain Monte Carlo (MCMC) simulation for parameter estimation and exploration of the posterior distribution of Bayesian models.

- **Hubble Dataset** : The observational value of the Hubble parameters give information about the expansion of the Universe. For finding our Hubble parameter we are using thirty-one data points which is obtained by the cosmic chronometers (CC), also known as the differential age technique, which is independent of the fiducial model. This technique was proposed by Jimenez and Loeb in [42]. The basic idea of this technique involve the measurement of age difference between two passively evolving early type galaxies by assuring that they are formed at the same time but with small difference at the redshift interval i.e. $\left(\frac{dz}{dt}\right)$. It provides us information about the Hubble function at various redshifts. We use thirty-one data points from redshift range between $0.07 < z < 1.965$. The corresponding χ_H^2 is given by

$$\chi_H^2(\Theta) = \sum_{i=1}^{31} \frac{((H(z_i, \Theta) - H_{obs}(z_i))^2}{\sigma_H^2(z_i)}. \quad (15)$$

Here $H(z_i, \Theta)$ is the theoretical value of Hubble parameter which we obtain from solving equation (14) and Θ represents the model parameters,

$H_{obs}(z_i)$ is the observed value of Hubble parameter of the corresponding redshift and $\sigma_H(z_i)$ is the observational error.

The Hubble dataset [43] is given below which is used for the analysis of the behaviour of the numerical solution of Eq. (14)

- **Pantheon⁺ Data** : The dataset consists of compilation of 1701 light curves of 1550 distinct Type Ia supernovae (SNe Ia) with relative luminosity distance ranging from $z = 0.00122$ to 2.2613 [44]. The magnitudes of parameters such as (stretch of the light curve, the colour at the maximum brightness and the stellar mass of the host galaxy) provided data is free from the systematic errors. We can write the the values of the distance moduli as,

$$\mu(z_i, \Theta) = 5 \log_{10}[D_L(z_i, \Theta)] + M, \quad (16)$$

where M is the absolute luminosity distance of a known star also act as a nuisance parameter in our MCMC simulation, it is added since the apparent magnitude of each luminosity distance needs to be calibrated. The corresponding luminosity distance D_L at each corresponding redshift z_i can be written as,

$$D_L(z_i, \Theta) = c(1 + z_i) \int_0^{z_i} \frac{dz'}{H(z', \Theta)}, \quad (17)$$

where H is the Hubble parameter which we will be estimating using MCMC simulation. The corresponding χ_{SN}^2 can be written as,

$$\chi_{SN}^2(\Theta) = (\Delta\mu(z_i, \Theta))^T C_{SN}^{-1} \Delta\mu(z_i, \Theta) + \ln \left(\frac{S}{2\pi} \right) - \frac{k^2(\Theta)}{S}, \quad (18)$$

where C_{SN} is the total covariance matrix, S is the sum of all the components of C_{SN}^{-1} and

$$k(\Theta) = \left(\mu(z_i, \Theta) - \mu_{obs}(z_i) \right)^T C_{SN}^{-1}.$$

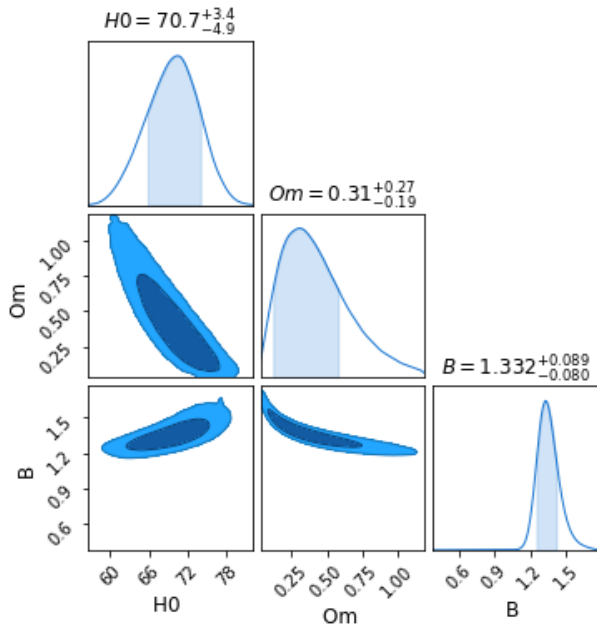
Markov Chain Monte Carlo (MCMC) analysis is used to constrain the model parameters using the above mentioned datasets and χ^2 minimization technique. The constrained values will be useful in interpreting various cosmological behaviour. We have assumed the value of $\alpha = 0.01$. MCMC is used to obtain the posterior distribution of parameters from a complex probability distributions using the observational data and a prior distribution idea. FIG.- 1 corner plot shows the joint and marginal distributions of the model parameters. The diagonal elements of the plots shows the marginal distribution of each model parameters, the sharpness and

width of each plot represents the well constrained and uncertainty in constraining the parameter values. The off diagonal plots shows the joint distribution of the parameters, elliptical contours of this plots shows the correlation between the parameters. The blue and light blue region of the joint distribution plots shows the 2σ and 1σ confidence level. FIG.- 1a and FIG.- 1b shows the constrained corner plot of the model parameters using Hubble data and Hubble+Pantheon⁺ data respectively. The constrained parameter values are given in TABLE - I.

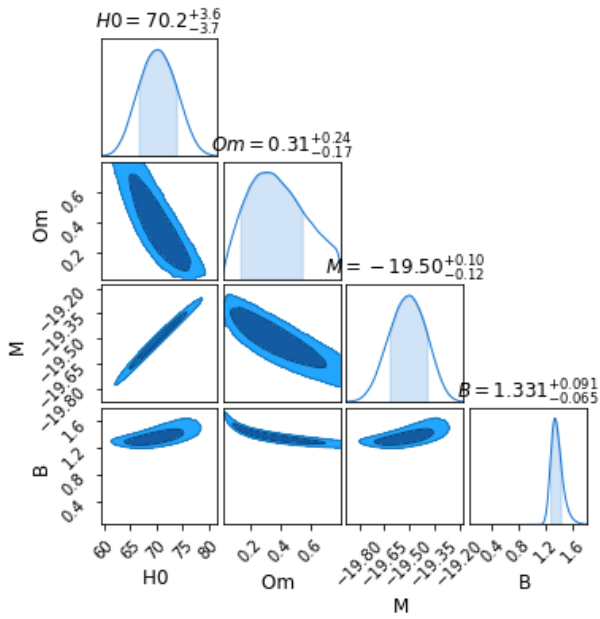
TABLE I: Constrained cosmological parameter values from different datasets

Parameter	Hubble Data	Hubble + Pantheon ⁺ Data
H_0	$70.7^{+3.4}_{-4.9}$	$70.2^{+3.6}_{-3.7}$
Ω_{m0}	$0.31^{+0.27}_{-0.19}$	$0.31^{+0.24}_{-0.17}$
M	-	$-19.50^{+0.10}_{-0.12}$
β	$1.332^{+0.089}_{-0.080}$	$1.331^{+0.091}_{-0.065}$

Using the constrained model parameter values from TABLE - I we can check the viability of the cosmological model mentioned in Eq. (11) in comparison with the standard Λ CDM model. In FIG.- 2 we have plotted errorbar plot of Hubble parameter $H(z)$ with redshift (z) using Hubble data points from TABLE- II. The dotted green lines represent the Λ CDM and solid red line is for the model with constrained parameter values from TABLE- I. The plot shows deviation of the model behaviour from Λ CDM with increase in redshift value. We calculated the value of distance modulus from Hubble parameter value using equation (16) and (17) and see the variation of distance modulus with redshift. FIG.- 3 is the plot for distance modulus $\mu(z)$ vs redshift (z) with errorbar plot using the Pantheon⁺ dataset [44]. The solid red line which passes through the error bars is for the assumed model with constrained model parameter values and dotted green lines is for the Λ CDM model. In both FIG.- 2 and FIG.- 3 we obtained the plots by considering the model parameter values as $H_0 = 70$, $\Omega_{m0} = 0.3$ and $\beta = 1.3$. In FIG.- 3, the error bars are plotted with corrected value of $M = +19.5$ both the plots shows a compatible behaviour of the model with Λ CDM with slight deviation as the value of redshift increases.



(a) Using Hubble datasets



(b) Using Hubble+Pantheon+ datasets

FIG. 1: Corner plots of constrained model parameters using (a) Hubble datasets on **upper panel** (b) combined Hubble and Pantheon+ datasets on **lower panel**

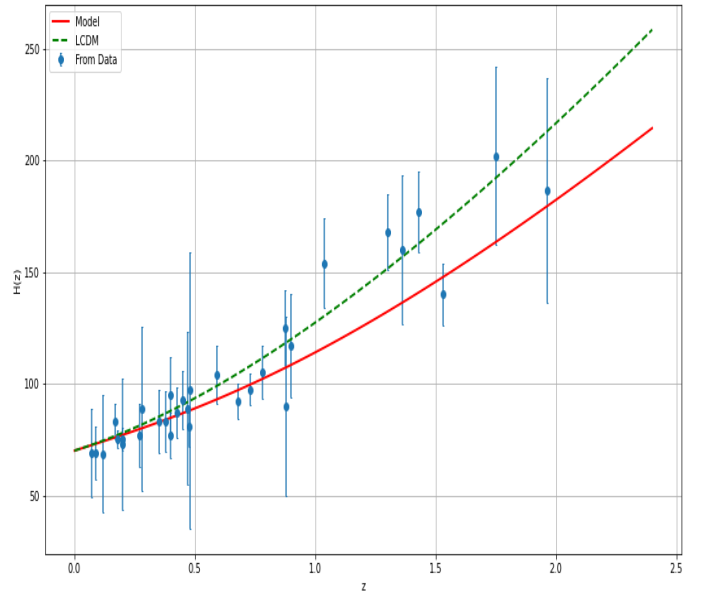


FIG. 2: $H(z)$ vs redshift plot with errorbars from the Hubble data points in TABLE- II. The solid red line is for the model and the dotted green line for the Λ CDM with errorbar plots for the 32 Hubble data points

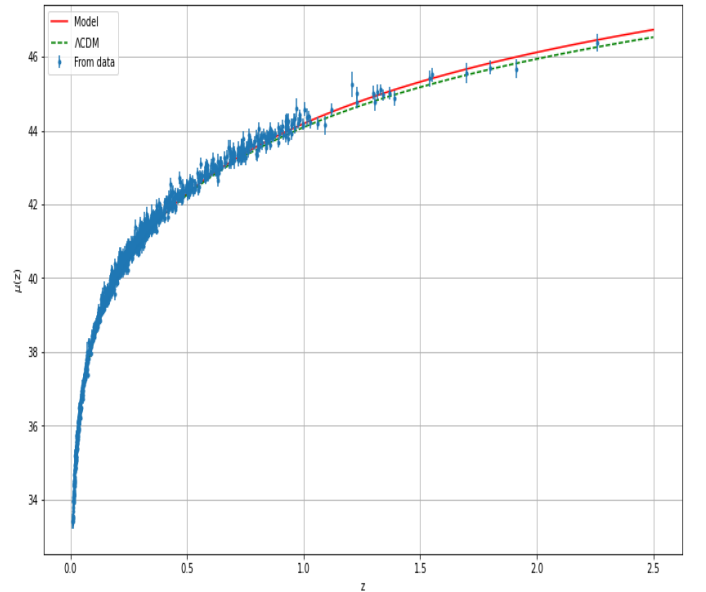


FIG. 3: $\mu(z)$ vs redshift with error bar plot using Pantheon+ data. The red line is for the model and the green dotted is the plot for Λ CDM.

IV. COSMOGRAPHIC PARAMETERS

According to the cosmological principle, the scale factor seems to be the only degree of freedom governing

the Universe. We may expand the scale factor $a(t)$ in a Taylor series around a_0 as [45–49],

$$a(t) = a_0 + \sum_{n=0}^{\infty} \frac{1}{n!} \frac{d^n a}{dt^n} \Big|_{(t=t_0)} (t - t_0)^n, \quad (19)$$

where t_0 is the present cosmic time and $n = 1, 2, 3, \dots$ is an integer. The coefficients of expansion are referred to as the cosmographic coefficients. In fact, the cosmographic coefficients contain different order of derivatives of the scale factor and therefore may provide a better geometrical description of the model. At any time t , we may define some geometrical parameters as,

$$H = \frac{\dot{a}}{a}, \quad q = -\frac{a\ddot{a}}{\dot{a}^2}, \quad j = \frac{\ddot{a}}{aH^3}, \quad s = \frac{a^{(4)}}{aH^4},$$

where $a^{(4)}$ is the fourth order derivatives of the scale factor. An integral part of the evolution of the Universe is the Hubble parameter H , which indicates how rapidly it is expanding. It is necessary to have a positive Hubble parameter if the Universe expands. The negative and positive signs of the deceleration parameter respectively provide information about the acceleration and deceleration of the Universe. These parameters can be expressed in redshift by using (14) as,

$$\begin{aligned} q(z) &= -1 + \frac{(1+z)H'(z)}{H(z)}, \\ j(z) &= 2q(z)^2 + q(z) + (1+z)q'(z), \\ s(z) &= \frac{j(z) - 1}{3\left(q(z) - \frac{1}{2}\right)}, \quad q \neq \frac{1}{2}. \end{aligned} \quad (20)$$

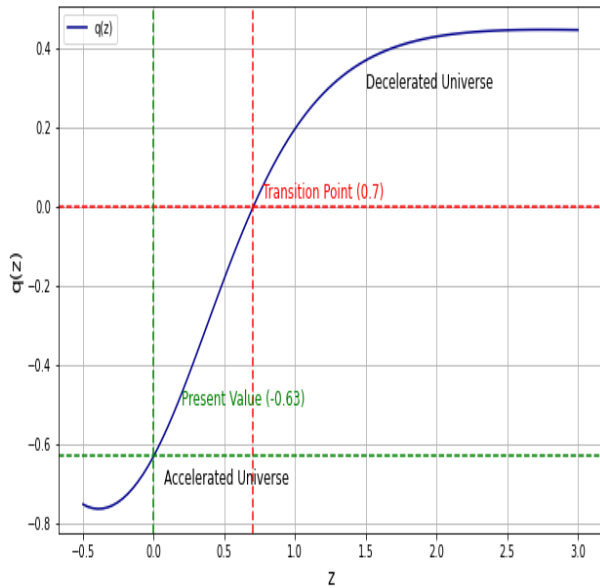


FIG. 4: Behaviour of deceleration parameter in redshift.

The value of q (with q_0 representing the present value) dictates the behavior of the Universe as: a decelerating, expanding Universe occurs when $q_0 > 0$, characteristic of a pressure-less barotropic fluid or matter-dominated Universe, likely representing the early Universe, though current observations do not support a positive q_0 . The current state of the Universe is an expanding and accelerating one, corresponding to $-1 < q_0 < 0$. A value of $q_0 = -1$ indicates a Universe dominated by a de Sitter fluid, relevant to the inflationary period of the very early Universe. From Eq. (20), the present value of the jerk parameter j_0 , is given by $j_0 = 2q_0^2 + q_0 + q_0'$. We consider $-1 < q_0 < -0.5$, which requires $2q_0^2 + q_0 > 0$. Thus, if $q_0 < -0.5$, j_0 depends on the sign of the variation of q . In other words, when j_0 is negative, the Universe remains in its present accelerated phase without any change, suggesting that dark energy has consistently influenced the dynamics since the dawn of time. Acceleration parameter stabilizes smoothly at a precise value when j_0 is zero. When j_0 is positive, there was a distinct point in the evolution of the Universe when acceleration began, marking a transition redshift where influence of dark energy became significant. The expansion of the Universe slope changes with the sign of j_0 , which suggests additional cosmological factors. Measuring the transition redshift z_{tr} directly is crucial to constraining the dark energy equation of state.

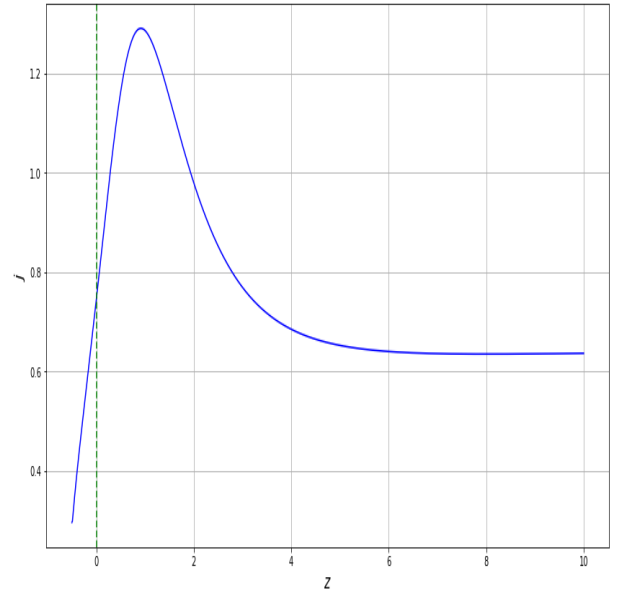


FIG. 5: Behaviour of jerk parameter in redshift.

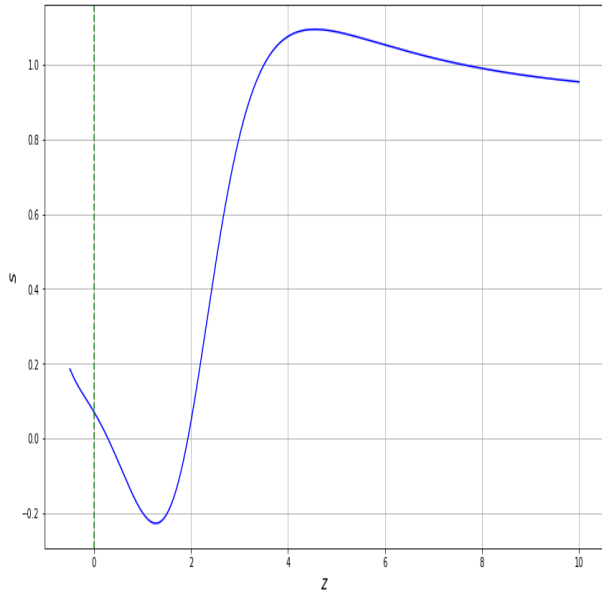


FIG. 6: Behaviour of snap parameter in redshift.

It is necessary to study the dynamics of deceleration parameter in order to understand the expansion nature of the Universe. In FIG.- 4 we have plotted the change in deceleration parameter with respect to redshift using the constrained parameter values in TABLE- I from Hubble and Hubble+Pantheon⁺ dataset as they give almost the same constrained parameter values. As mentioned above for an expanding Universe, Hubble parameter has to be positive and from the formula of $q(z)$ in Eq. (20) we can say that $q(z)$ has to be negative. In the FIG.- 4, $z = 0$ indicates the present time of the Universe and the value of $q(z)$ is $q_0 = -0.63$ shows the accelerating phase of the Universe. The recently performed measurements have determined that the value of the deceleration parameter for the current cosmic epoch is within the range of $q_0 = -0.528^{+0.092}_{-0.088}$ [46] and transition from deceleration to acceleration at $z_t = 0.60^{+0.21}_{-0.12}$ [50, 51]. As we can see from FIG.- 4, the deceleration parameter shows early deceleration to late time acceleration, where as the transition happens at $z_t = 0.70$. In FIG.- 5, we have plotted the jerk parameter(j) with respect to redshift, jerk parameter is a dimensionless parameter obtained from the coefficient fourth term in Eq. (19). From Fig.- 5 we can see the dynamical nature of the model showing constant rate of acceleration expansion of the Universe at early time. At late times, time varying acceleration with ($j > 0$) indicating increasing acceleration expansion, similar to the behavior of Λ CDM model. We have also studied the ($s - z$) plot in FIG.- 6 to understand more about the model description of dynamics of dark energy. We can observe that $s > 0$ at early time

shows the quintessence phase of the Universe and the trajectory of the plot converges to Λ CDM in late time with $s = 0$ which again explain the accelerating expansion behaviour of the Universe.

V. TEST FOR THE VALIDATION

The validity of any cosmological model can be checked through some theoretical and observational tests. In this discussion, we will examine several cosmological tests that may be employed to authenticate our derived model. Also calculated the age of the Universe to validate the model.

EoS Parameter : Describes the relationship between cosmic fluid pressure and energy density using the equation of state (EoS) parameter. Generally represented as ω , this parameter governs the expansion of the Universe and provides insight into its evolution stages. The value of ω may deviate from the standard cosmological constant case ($\omega = -1$), indicating exotic behaviors such as phantom energy ($\omega < -1$) or quintessence ($-1 < \omega < -1/3$). Understanding the EoS parameter in this gravity is essential for predicting the fate of the Universe whether it will experience accelerated expansion or deceleration in current cosmological research and observational studies.

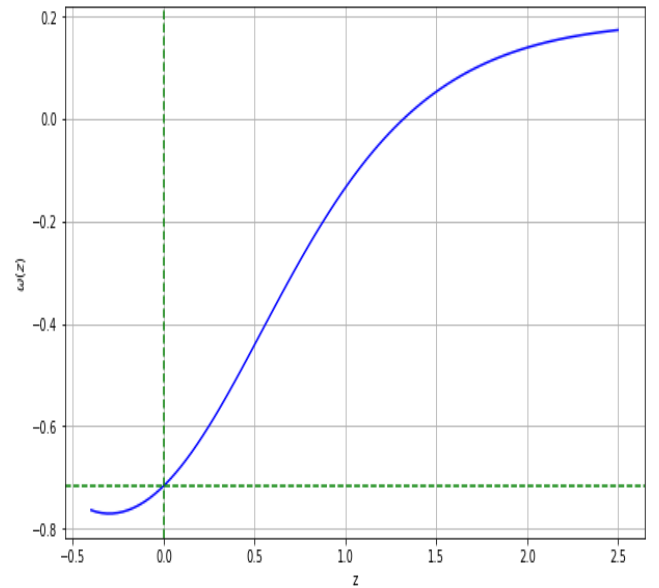


FIG. 7: Behaviour of EoS parameter in redshift.

Using the Eq. (10) and Eq. (14), the EoS parameter can be expressed. FIG.- 7 illustrates the dynamic nature of ω that can change significantly from an early to a late epoch. With the value of $\omega = -0.72$ at $z = 0$, the EoS

parameter shows the quintessence behavior at present and converges to Λ CDM in late time.

Statefinder Diagnostic : The state finder pair (j, s) characterizes the properties of dark energy in the model independent manner. Sahni et al [52, 53] have proposed this diagnostic with the classification: (i) $(j = 1, s = 0)$ corresponds to the Λ CDM model, (ii) $(j < 1, s > 0)$ indicates Quintessence, (iii) $(j > 1, s < 0)$ represents Chaplygin Gas, and (iv) $(j = 1, s = 1)$ signifies SCDM. So, the state finder pair helps to distinguish different dark energy models.

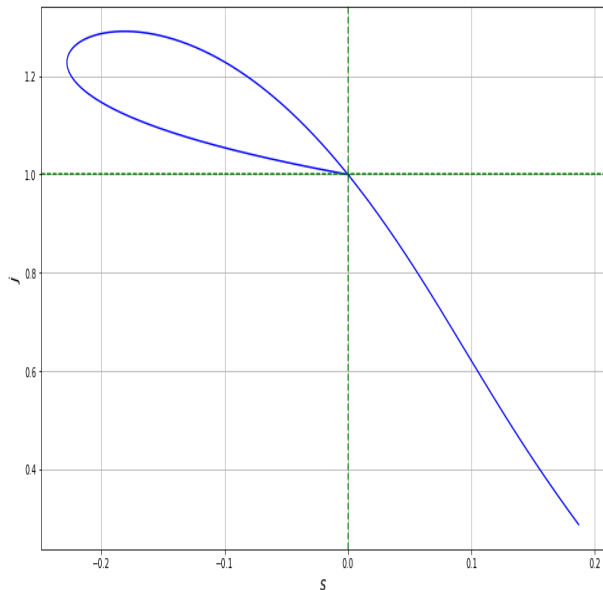


FIG. 8: Behaviour of state finder pair in redshift.

One can see the behaviour of the state finder pair in FIG.- 8, which is used to determine different dark energy model of the expansion Universe. In this method j and s are the two diagnostic parameters, the j -parameter gives us the rate of change in acceleration or deceleration of the Universe while the s -parameter helps in distinguishing different dark energy model. From this plot we can see the dynamics of the model with the constrained parameter values from the dataset, in early time the model shows Quintessence behaviour with $(j < 1)$ for $(s > 0)$ and the $j - s$ pair converges to Λ CDM in the late time at the fix point where $(s = 0)$ and $(j = 1)$ which shows the late time accelerating expanding behaviour of the Universe.

$Om(z)$ Diagnostic : The $Om(z)$ diagnostic has been introduced as an alternative approach to test the accelerated expansion of the Universe with the phenomenological assumption, EoS, $p = \rho\omega$ filling the Universe with

the perfect fluid. This diagnostic tool distinguishes the standard Λ CDM model from other dark energy models such as quintessence and phantom. Also, there are evidences available in the literature on its sensitiveness with the EoS parameter [54–56]. The nature of $Om(z)$ slope differs between dark energy models because: the positive slope indicates the phantom phase $\omega < -1$, and the negative slope indicates the quintessence region $\omega > -1$. The $Om(z)$ diagnostic can be defined as,

$$Om(z) = \frac{E^2(z) - 1}{(1+z)^3 - 1}, \quad E(z) = \frac{H(z)}{H_0}$$

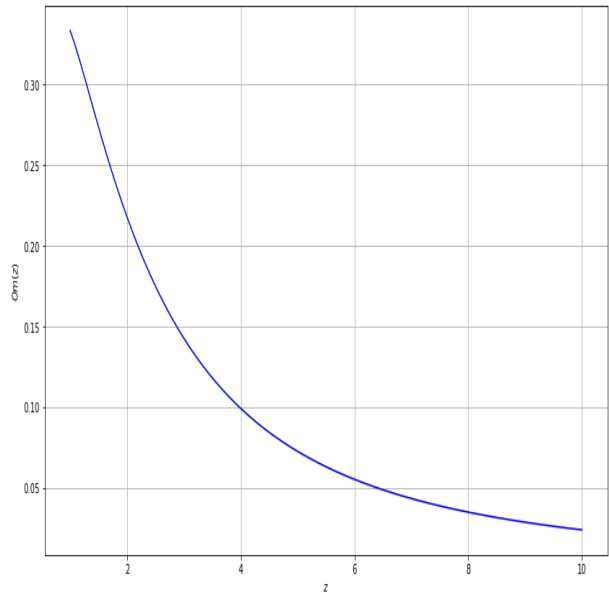


FIG. 9: Behaviour of $Om(z)$ in redshift.

In FIG.- 9, the growth of $Om(z)$ has been illustrated which shows that at later stages, it tends to support the viability of decaying dark energy models (quintessence dark energy at late time).

Age of the Universe : We can also calculate the age of the Universe using Hubble time as discussed in [57]. The age of the Universe as any value of redshift (z) is given by

$$t_U(z) = \int_z^\infty \frac{d\tilde{z}}{(1+\tilde{z})H(\tilde{z})}.$$

The present age of the Universe is given by the reciprocal of the Hubble constant $H_0 = H(z = 0)$. We can compute the value of age of Universe using the numerically calculated value Hubble parameter from (12) and

the below formula

$$H_0 t_0 = \lim_{z \rightarrow \infty} \int_0^z \frac{d\tilde{z}}{(1+\tilde{z})E(\tilde{z})},$$

$$t_0 = \left[\int_0^z \frac{d\tilde{z}}{(1+\tilde{z})E(\tilde{z})} \right] \times \left(\frac{1}{H_0} \right)$$

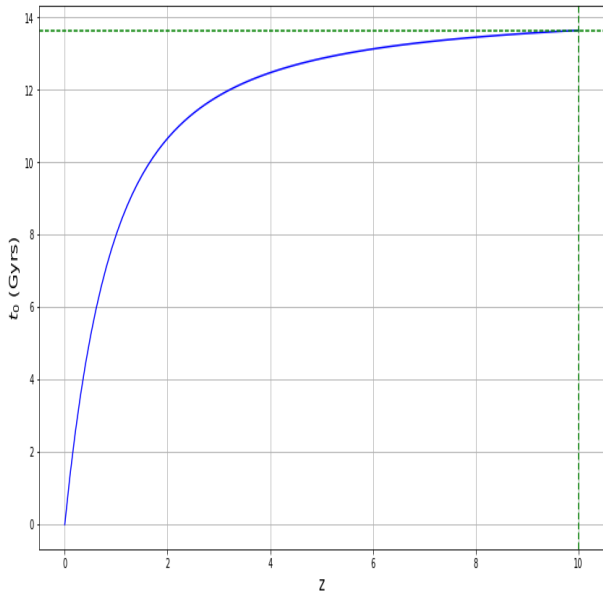


FIG. 10: Hubble time $t_U(z)$ in redshift in terms of years.

In FIG.- 10 we have plotted age of the Universe in terms of years with respect to redshift. At a very large value of redshift the age of the Universe calculated from Hubble time is converging in $t_0 \approx 13.64$ Gyrs, quite close to the age calculated from the Planck result $t_0 = 13.78 \pm 0.020$ Gyrs. So, the results obtained in the model are in consistent with the present prescribed value according to cosmological observations.

VI. CONCLUSION

In this work, we have considered a functional form of the type $f(R) + f(\mathcal{L}_m)$ in the $f(R, \mathcal{L}_m)$ gravity, which is extension of the $f(R)$ gravity. The functional form of the $f(R, \mathcal{L}_m)$ is inspired from the Starobinsky model in $f(R)$ gravity theory and $f(\mathcal{L}_m)$ from powerlaw model and studied the dynamics of Universe using $f(R, \mathcal{L}_m)$ gravity theory. After calculating the field equation for $f(R, \mathcal{L}_m)$ using the gravitational action, the parametrized $H(z)$ is obtained using the field equations and the flat FLRW metric space time. Due to complexity of the differential equation for $H(z)$, the solution is obtained numerically for the $H(z)$.

The MCMC analysis is used to estimate the free model parameters through the 32 Hubble data points in the range $0.07 < z < 1.965$ and the 1701 Pantheon⁺ data points (light curves) in the range $0.00122 < z < 2.2613$ and the χ^2 minimization technique. The constrained parameter values are shown in Table-I with the $1 - \sigma$ confidence error. The comparison between the numerical solution for $H(z)$ and the Λ CDM model using error bar plots for Hubble data set and Pantheon⁺ data set has been done. Moreover the geometrical parameters have been calculated. The present value for the deceleration parameter is obtained as $q_0 \approx -0.63$, where the transition from deceleration to acceleration happens at the point $z_t \approx 0.70$. Whereas the present values for jerk parameter [$j_0 =$] and snap parameter [$s_0 =$] shows the quintessence behaviour of the model at present epoch.

We have calculated the EoS parameter for the model, which gives present value $\omega_0 = -0.72$ showing the quintessence phase of the Universe. Also, we performed state finder diagnostic and $Om(z)$ diagnostic validation tests to the viability of the model. We obtained that the dynamics of the model shifting from early time quintessence phase and converging to late time Λ CDM model using state finder diagnostics. Moreover the $Om(z)$ diagnostics favors to the quintessence behaviour of the model. Finally we have calculated the age of the Universe using Hubble time and according to the model we have assumed the present age of the Universe is coming out to be $t_0 \approx 13.64$ Gyrs which is close to the calculated value from the Planck i.e $t_0 = 13.78 \pm 0.020$ Gyrs. So, overall this model shows a viable behaviour and consistent value with the observed data sets.

ACKNOWLEDGEMENT

BM acknowledges the support of Council of Scientific and Industrial Research (CSIR) for the project grant (No. 03/1493/23/EMR II).

APPENDIX

TABLE II: The observational Hubble dataset.

<i>Sr.No.</i>	<i>Redshift (z)</i>	<i>H(z) [km/s/Mpc]</i>	σ_H [km/s/Mpc]	<i>Sr.No.</i>	<i>Redshift (z)</i>	<i>H(z) [km/s/Mpc]</i>	σ_H [km/s/Mpc]
1	0.07	69.0	19.6	17	0.4783	80.9	9.0
2	0.09	69.0	12.0	18	0.48	97.0	62.0
3	0.12	68.6	26.2	19	0.593	104.0	13.0
4	0.17	83.0	8.0	20	0.68	92.0	8.0
5	0.179	75.0	4.0	21	0.75	98.8	33.6
6	0.199	75.0	5.0	22	0.781	105.0	12.0
7	0.20	72.9	29.6	23	0.875	125.0	17.0
8	0.27	77.0	14.0	24	0.88	90.0	40.0
9	0.28	88.8	36.6	25	0.9	117.0	23.0
10	0.352	83.0	14.0	26	1.037	154.0	20.0
11	0.38	83.0	13.5	27	1.3	168.0	17.0
12	0.4	95.0	17.0	28	1.363	160.0	14.0
13	0.4004	77.0	10.2	29	1.43	177.0	40.0
14	0.425	87.1	11.2	30	1.53	140.0	18.0
15	0.445	92.8	12.9	31	1.75	202.0	14.0
16	0.47	89.0	49.6	32	1.965	186.5	50.4

REFERENCES

- [1] C.L. Bennett, M. Halpern, G. Hinshaw, N. Jarosik et al., *First-Year Wilkinson Microwave Anisotropy Probe (WMAP)* Observations: Preliminary Maps and Basic Results*, *Astrophys. J. Supp. Ser.* **148** (2003) 1.
- [2] D.N. Spergel, L. Verde, H.V. Peiris, E. Komatsu et al., *First-Year Wilkinson Microwave Anisotropy Probe (WMAP)* Observations: Determination of Cosmological Parameters*, *Astrophys. J. Supp. Ser.* **148** (2003) 175.
- [3] D.N. Spergel, R. Bean, O. Doré, M.R. Nolta et al., *Three-Year Wilkinson Microwave Anisotropy Probe (WMAP) Observations: Implications for Cosmology*, *Astrophys. J. Supp. Ser.* **170** (2007) 377.
- [4] S. Perlmutter, S. Gabi, G. Goldhaber, A. Goobar et al., *Measurements* of the Cosmological Parameters Ω and Λ from the First Seven Supernovae at $z \geq 0.35$* , *Astrophys. J.* **483** (1997) 565.
- [5] S. Perlmutter, G. Aldering, M.D. Valle, S. Deustua et al., *Discovery of a supernova explosion at half the age of the Universe*, *nature* **391** (1998) 51.
- [6] S. Perlmutter, G. Aldering, G. Goldhaber, R.A. Knop et al., *Measurements of Ω and Λ from 42 High-Redshift Supernovae*, *Astrophys. J.* **517** (1999) 565.
- [7] A.G. Riess, L.-G. Strolger, J. Tonry, S. Casertano et al., *Type Ia Supernova Discoveries at $z > 1$ from the Hubble Space Telescope: Evidence for Past Deceleration and Constraints on Dark Energy Evolution**, *Astrophys. J.* **607** (2004) 665.
- [8] A.G. Riess, L.-G. Strolger, S. Casertano, H.C. Ferguson et al., *New Hubble Space Telescope Discoveries of Type Ia Supernovae at $z \geq 1$: Narrowing Constraints on the Early Behavior of Dark Energy**, *Astrophys. J.* **659** (2007) 98.
- [9] E. Hawkins, S. Maddox, S. Cole, O. Lahav et al., *The 2dF Galaxy Redshift Survey: correlation functions, peculiar velocities and the matter density of the Universe*, *Mon. Notices Royal Astron. Soc.* **346** (2003) 78.
- [10] M. Tegmark, M.A. Strauss, M.R. Blanton, K. Abazajian et al., *Cosmological parameters from sdss and wmap*, *Phys. Rev. D* **69** (2004) 103501.
- [11] S. Cole, W.J. Percival, J.A. Peacock, P. Norberg et al., *The 2dF Galaxy Redshift Survey: power-spectrum analysis of the final data set and cosmological implications*, *Mon. Notices Royal Astron. Soc.* **362** (2005) 505.
- [12] D.J. Eisenstein, I. Zehavi, D.W. Hogg, R. Scoccimarro et al., *Detection of the Baryon Acoustic Peak in the Large-Scale Correlation Function of SDSS Luminous Red Galaxies*, *Astrophys. J.* **633** (2005) 560.
- [13] S. Nojiri and S.D. Odintsov, *Introduction to modified gravity and gravitational alternative for dark energy*, *Int. J. Geom. Methods Mod. Phys.* **04** (2007) 115.

- [14] S. Capozziello and M. De Laurentis, *Extended theories of gravity*, *Phys. Rep.* **509** (2011) 167.
- [15] E.N. Saridakis, R. Lazkoz, V. Salzano, P.V. Moniz et al., *Modified Gravity and Cosmology: An Update by the CANTATA Network*, Springer Cham (2021), [10.1007/978-3-030-83715-0](https://doi.org/10.1007/978-3-030-83715-0).
- [16] K.S. Stelle, *Renormalization of higher-derivative quantum gravity*, *Phys. Rev. D* **16** (1977) 953.
- [17] A.G. Riess, A.V. Filippenko, P. Challis, A. Clocchiatti et al., *Observational Evidence from Supernovae for an Accelerating Universe and a Cosmological Constant*, *Astron. J.* **116** (1998) 1009.
- [18] M. Betoule, R. Kessler, J. Guy, J. Mosher et al., *Improved cosmological constraints from a joint analysis of the SDSS-II and SNLS supernova samples*, *Astron. Astrophys.* **568** (2014) A22.
- [19] P.A.R. Ade, N. Aghanim, M. Arnaud, M. Ashdown et al., *Planck 2015 results - XIII. Cosmological parameters*, *Astron. Astrophys.* **594** (2015) A13.
- [20] N. Aghanim, M. Arnaud, M. Ashdown, J. Aumont et al., *Planck 2015 results - XI. CMB power spectra, likelihoods, and robustness of parameters*, *Astron. Astrophys.* **594** (2016) A11.
- [21] S.M. Carroll, V. Duvvuri, M. Trodden and M.S. Turner, *Is cosmic speed-up due to new gravitational physics?*, *Phys. Rev. D* **70** (2004) 043528.
- [22] W. Hu and I. Sawicki, *Models of $f(R)$ cosmic acceleration that evade solar system tests*, *Phys. Rev. D* **76** (2007) 064004.
- [23] I. Sawicki and W. Hu, *Stability of cosmological solutions in $f(R)$ models of gravity*, *Phys. Rev. D* **75** (2007) 127502.
- [24] L. Amendola and S. Tsujikawa, *Phantom crossing, equation-of-state singularities, and local gravity constraints in $f(R)$ models*, *Phys. Lett. B* **660** (2008) 125.
- [25] S. Capozziello, P. Martin-Moruno and C. Rubano, *Dark energy and dust matter phases from an exact $f(R)$ -cosmology model*, *Phys. Lett. B* **664** (2008) 12.
- [26] S. Nojiri and S.D. Odintsov, *Introduction to Modified Gravity and Gravitational Alternative for Dark Energy*, *Int. J. Geom. Methods Mod. Phys.* **4** (2007) 115.
- [27] T. Multamäki and I. Vilja, *Spherically symmetric solutions of modified field equations in $f(R)$ theories of gravity*, *Phys. Rev. D* **74** (2006) 064022.
- [28] T. Multamäki and I. Vilja, *Static spherically symmetric perfect fluid solutions in $f(R)$ theories of gravity*, *Phys. Rev. D* **76** (2007) 064021.
- [29] M.F. Shamir, *Some Bianchi type cosmological models in $f(R)$ gravity*, *Astrophys. and Space Sci.* **330** (2010) 183.
- [30] Santos, J. and Alcaniz, J. S. and Rebouças, M. J. and Carvalho, F. C., *Energy conditions in $f(R)$ gravity*, *Phys. Rev. D* **76** (2007) 083513.
- [31] O. Bertolami, C.G. Böhrer, T. Harko and F.S.N. Lobo, *Extra force in $f(R)$ modified theories of gravity*, *Phys. Rev. D* **75** (2007) 104016.
- [32] T. Harko, *Modified gravity with arbitrary coupling between matter and geometry*, *Phys. Lett. B* **669** (2008) 376.
- [33] T. Harko and F.S. Lobo, *$f(R, L_m)$ gravity*, *Eur. Phys. J. C* **70** (2010) 373.
- [34] T. Harko, *Galactic rotation curves in modified gravity with nonminimal coupling between matter and geometry*, *Phys. Rev. D* **81** (2010) 084050.
- [35] T. Harko, *The matter Lagrangian and the energy-momentum tensor in modified gravity with nonminimal coupling between matter and geometry*, *Phys. Rev. D* **81** (2010) 044021.
- [36] S. Nesseris, *Matter density perturbations in modified gravity models with arbitrary coupling between matter and geometry*, *Phys. Rev. D* **79** (2009) 044015.
- [37] V. Faraoni, *Viability criterion for modified gravity with an extra force*, *Phys. Rev. D* **76** (2007) 127501.
- [38] V. Faraoni, *Lagrangian description of perfect fluids and modified gravity with an extra force*, *Phys. Rev. D* **80** (2009) 124040.
- [39] B. Gonçalves, P. Moraes and B. Mishra, *Cosmology from Non-Minimal Geometry-Matter Coupling*, *Fortschritte der Phys.* **71** (2023) 2200153.
- [40] A. Starobinsky, *A New Type of Isotropic Cosmological Models Without Singularity*, *Phys. Lett. B* **91** (1980) 99.
- [41] T. Harko and F. Lobo, *Generalized Curvature-Matter Couplings in Modified Gravity*, *Galaxies* **2** (2014) 410.
- [42] R. Jimenez and A. Loeb, *Constraining Cosmological Parameters Based on Relative Galaxy Ages*, *Astrophys. J.* **573** (2002) 37.
- [43] S.A. Narawade and B. Mishra, *Phantom Cosmological Model with Observational Constraints in $f(Q)$ Gravity*, *Annalen Phys.* (2023) 2200626.
- [44] D. Brout, D. Scolnic, B. Popovic, A.G. Riess et al., *The Pantheon⁺ Analysis: Cosmological Constraints*, *Astrophys. J.* **938** (2022) 110.
- [45] A. Aviles, C. Gruber, O. Luongo and H. Quevedo, *Cosmography and constraints on the equation of state of the Universe in various parametrizations*, *Phys. Rev. D* **86** (2012) 123516.
- [46] C. Gruber and O. Luongo, *Cosmographic analysis of the equation of state of the universe through Padé approximations*, *Phys. Rev. D* **89** (2014) 103506.
- [47] S. Weinberg and R.V. Wagoner, *Gravitation and Cosmology: Principles and Applications of the General Theory of Relativity*, *Phys. Today* **26** (1973) 57.
- [48] M. Visser, *Jerk, snap and the cosmological equation of state*, *Class. Quant. Grav.* **21** (2004) 2603.
- [49] M. Visser, *Cosmography: Cosmology without the Einstein equations*, *Gen. Relativ. Gravit.* **37** (2005) 1541.
- [50] Y. Yang and Y. Gong, *The evidence of cosmic acceleration and observational constraints*, *JCAP* **2020** (2020) 059.
- [51] S. Capozziello, O. Luongo and E.N. Saridakis, *Transition redshift in $f(T)$ cosmology and observational constraints*, *Phys. Rev. D* **91** (2015) 124037.
- [52] V. Sahni, T.D. Saini, A.A. Starobinsky and U. Alam, *Statefinder-A new geometrical diagnostic of dark energy*, *J. Exp. Theor. Phys.* **77** (2003) 201.
- [53] U. Alam, V. Sahni, T. Deep Saini and A.A. Starobinsky, *Exploring the expanding Universe and dark energy using the statefinder diagnostic*, *Mon. Notices Royal Astron. Soc.* **344** (2003) 1057.
- [54] X. Ding, M. Biesiada, S. Cao, Z. Li and Z.-H. Zhu, *Is there evidence for dark energy evolution?*, *Astrophys. J. Lett.* **803**

- (2015) L22.
- [55] X. Zheng, X. Ding, M. Biesiada, S. Cao and Z.-H. Zhu, *What are the $\Omega_m h^2(z_1, z_2)$ and $\Omega_m(z_1, z_2)$ diagnostics telling us in light of $H(z)$ data?*, *Astrophys. J.* **825** (2016) 17.
- [56] J.-Z. Qi, S. Cao, M. Biesiada, T.-P. Xu, Y. Wu, S.-X. Zhang et al., *What do parameterized $\Omega_m(z)$ diagnostics tell us in light of recent observations?*, *Res. Astron. Astrophys.* **18** (2018) 066.
- [57] S. Vagnozzi, F. Pacucci and A. Loeb, *Implications for the Hubble tension from the ages of the oldest astrophysical objects*, *J. High Energy Phys.* **36** (2022) 27.